Adv. Space Res. Vol. 8, No. 9–10, pp. (9)281–(9)299, 1988
Printed in Great Britain. All rights reserved.
0273–1177/88 $0.00 + .50
Copyright © 1989 COSPAR

OBSERVATIONS AT THE MAGNETOPAUSE AND IN THE AURORAL IONOSPHERE OF MOMENTUM TRANSFER FROM THE SOLAR WIND

M. Lockwood* and S. W. H. Cowley**

*Rutherford Appleton Laboratory, Chilton, Didcot, Oxfordshire OX11 0QX, U.K.
**Blackett Laboratory, Imperial College, London, SW7 2BZ, U.K.

ABSTRACT

Recent radar studies of field-perpendicular flows in the auroral ionosphere, in conjunction with observations of the interplanetary medium immediately upstream of the Earth's bow shock, have revealed direct control of dayside convection by the B_z component of the interplanetary magnetic field (IMF). The ionospheric flows begin to respond to both northward and southward turnings of the IMF impinging upon the magnetopause after a delay of only a few minutes in the early afternoon sector, rising to about 15 minutes nearer dawn and dusk. In both the polar cap and the auroral oval, the subsequent rise and decay times are of order 5-10 minutes. We conclude there is very little convection "flywheel" effect in the dayside polar ionosphere and that only newly-opened flux tubes impart significant momentum to the ionosphere, in a relatively narrow region immediately poleward of the cusp. These findings concerning the effects of quasi-steady reconnection have important implications for any ionospheric signatures of transient reconnection which should be considerably shorter-lived than thought hitherto. In order to demonstrate the difficulty of uniquely identifying a Flux Transfer Event (FTE) in ground-based magnetometer data, we present observations of an impulsive signature, identical with that expected for an FTE if data from only one station is studied, following an observed magnetopause compression when the IMF was purely northward. We also report new radar observations of a viscous-like interaction, consistent with an origin on the flanks of the magnetotail and contributing an estimated 15-30kV to the total cross-cap potential during quiet periods.

INTRODUCTION

Only one set of observations has been made which directly show momentum transfer at the magnetopause and a response in ionospheric convection velocities. These multipoint measurements on 4 September, 1984 included: observations of the IMF by the ISEE 1 and 2 spacecraft; an inbound pass of AMPTE-IRM for which the stress-balance test demonstrates quasi-steady reconnection is occuring at an eroding magnetopause /1/; and observations by the SABRE coherent radar of the effects of the dayside open field line boundary moving equatorward /2/. For other sets of observations, a greater degree of inferrence is required. For example, combined observations by the STARE radar and the GEOS geostationary satellite have been shown to be consistent with momentum transfer by a Flux Transfer Event (FTE) /3/: however, the magnetopause observations were based on the lack of dispersion of particle 'drop-outs' at the satellite and usual magnetometer observations of an FTE /4/ were not available. In other studies, indirect evidence for convection changes, obtained for example from the A_L and A_E auroral magnetic indices, was compared with in-situ observations of magnetospheric erosion (e.g. /49/).

In the absence of direct observations of momentum transfer at the magnetopause, it must be inferred from comparison of flows and fields in the interplanetary medium and those inside the magnetosphere or in the ionosphere. In this paper, we do not intend to review the large number of studies which compare simultaneous observations of cross polar-cap potential and the IMF, as several extensive reviews on this subject are already available /5,6,7/. However, we note that cross-cap potential values from polar-orbiting satellites are a form of average over the period taken by the satellite to traverse the polar cap (15-60 minutes, depending on altitude); values from magnetometers have 5-minute resolution but employ spatial smoothing and assume distributions of ionospheric conductivities; and values from incoherent scatter radars are deduced from large latitude scans (typically taking 30 minutes) which are combined statistically. In this paper, we will report on important new findings from radars observing ionospheric convection with temporal resolutions down to 15 seconds. The results not only reveal ionospheric flows consistent with transient reconnection and viscous-like momentum transfer at the magnetopause, but also call for a radically new concept of the excitation of ionospheric plasma convection by quasi-steady reconnection. Table 1 lists some of the observatories and observing platforms which have been used to study momentum transfer from the magnetosheath to the magnetosphere by also observing its consequences in the ionosphere.

TABLE 1 Multipoint Observations of Momentum Transfer from the Solar Wind to the Magnetosphere and Ionosphere

Magnetopause process	Ground-Based Ionospheric Observatory	Polar-Orbiting Satellite	Magnetopause Observations	Solar Wind/IMF Monitor	References
a) Quasi-steady reconnection	EISCAT	-	-	AMPTE-UKS and -IRM	9,10,11,12,13 15,23
	Sondrestrom radar and magnetometers	-	-	IMP-8	24,25,47
	SABRE	-	AMPTE-UKS and -IRM	ISEE 2	1,2
	-	AE-C, DE-2, S3-2 or S3-3	-	IMP-8	5,6,7,16
	magnetometers	-	OGO -5	EXPLORER 33 or 35, HEOS 1	49
	magnetometers	-	-	IMP-1, 7 or 8	45,46
	magnetometers	DSMP F2 and P87-1	-	IMP-8	17
		DE-1 or VIKING imager	-	IMP-8	18,48
b) Transient Reconnection	EISCAT	-	-	AMPTE-UKS and -IRM	15,33
	STARE	-	GEOS	IMP-8	3
	Conjugate magnetometers	-	-	IMP-8	37,38
	Photometer	HILAT	-	IMP-8	36
c) Viscous-like interaction	magnetometers	AE-C, DE-2, S3-2 or S3-3	-	IMP-8	5,6,7,32
			ISEE-1 and -2	IMP-8	28,30,31
d) Dynamic Pressure Changes	magnetometers	-	-	IMP-8	40,41,42
	magnetometers	VIKING and AMPTE-CCE	-	IMP-8	43
	magnetometers	-	ISEE-1 and -2	IMP-8	44

OBSERVATIONS OF THE EFFECTS OF QUASI-STEADY RECONNECTION AT THE MAGNETOPAUSE

The basic quantity we wish to study in this section is the "ionospheric response time", T_{MR}. As illustrated in figure 1, this includes a delay T_{MC}, for information on any change in the rate of momentum exchange at the subsolar magnetopause (M) to reach the ionosphere (at the point C) and any further time, T_{CR}, for the effect to reach the field of view of an ionospheric observatory (R). We shall show that the latter contribution to the lag is due to the re-organisation of the ionospheric flow pattern and changes propagate at a speed V_{io} which is considerably slower than the field-perpendicular Alfvèn speed. Furthermore, the latter is so large that the ionosphere can be regarded, to a high degree of accuracy, as being incompressible. In order to compute the ionospheric response time, the propagation time of any perturbation in the interplanetary medium from the satellite to the bow shock, T_{SB}, and across the magnetosheath, T_{BM}, must be estimated using statistical models of bow shock and magnetopause positions and a gas-dynamic model of bow shock slowing of solar wind flow. In this paper, we will concentrate on interplanetary observations by the AMPTE-UKS and -IRM satellites when immediately upstream of the Earth's bow shock. These observations allow the propagation delays T_{SM} to be estimated with uniquely low error.

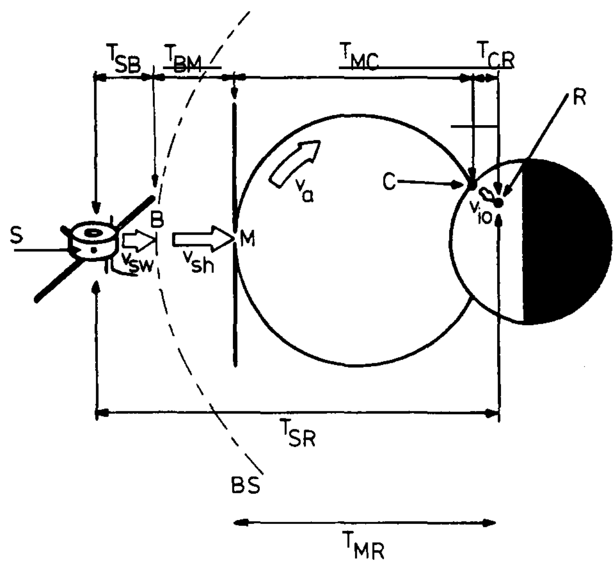

Fig. 1. Schematic of the propagation of a disturbance in the interplanetary medium to a region of the ionosphere: S is the interplanetary monitor satellite; B, M and C and the points first affected at the bow shock, magnetopause and ionosphere, respectively; R is the field-of-view of an ionospheric observatory. The propagation delay between X and Y is T_{XY} (from /11/).

We have compared these AMPTE observations with simultaneous measurements of the ionospheric plasma flow made by the UK-POLAR experiment on the EISCAT radar /8,9/. In this mode of operation, EISCAT produces 2.5-minute resolution vectors by the beamswinging technique and 15-second resolution line-of-sight velocities. Figure 2 shows an example of such simultaneous observations for the period 10:30 - 12:00 UT on 27th October, 1984, during which the IMF was observed to turn abruptly southward at 11:07 UT /9,10,11/. The bottom panel shows the flow vectors observed by EISCAT (in "electric field" format, i.e. with vectors pointing up the page corresponding to westward flow), superposed on colour-coded observed ion temperatures. A strong enhancement of the mid-afternoon auroral zone flow (MLT ≈ UT + 2.5 hrs. ≈ 14:00) is seen after a delay, $T_{SR} = 11 \pm 0.5$ min /9/, corresponding to an ionospheric response time, $T_{MR} = 5 \pm 1$ min /12/. These data show a very high degree of correlation between the IMF B_z component and the magnitude of the ionospheric flow /9/. However, there are also interesting differences between the response lags for the first and the (minor) second southward turnings, and both these also differ from that for the short-lived northward turning: these differences will be discussed and explained in the following section. The direct control of auroral ionospheric convection by IMF B_z was confirmed by a statistical survey of all the combined EISCAT-AMPTE data using the 2.5-minute flow vectors /13/. Examples of the cross-correlation functions obtained are shown on the left of figure 3, for three invariant latitudes and the same range of MLT (13-15 hrs). The correlation coefficient shows a strong peak at short lags for the dominant eastward flow component (negative lag meaning that the IMF leads the ionospheric flow). To the right of figure 3 are the scatter plots of the northward and eastward ionospheric flow components as a function of $(V_{sw}/500)^2 B_z$, where V_{sw} is the solar wind speed in km s^{-1}, for the lags giving the peak correlations shown to the left of the figure. It can be seen that the flow data are well-ordered by this combination of interplanetary variables, when the appropriate lag is employed, flow speeds being strongly dependent on B_z when $B_z < 0$ but small, much more scattered and independent of B_z when $B_z > 0$.

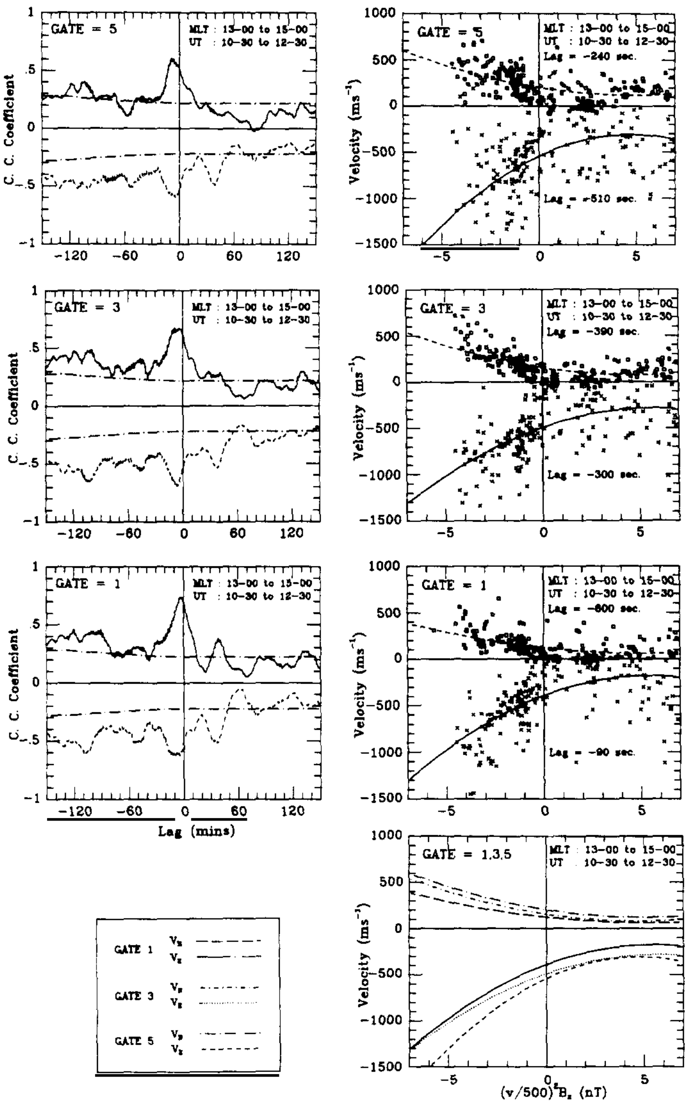

Fig. 3. Examples of cross-correlation coefficients as a function of lag (left) and scatter plots at the lag of peak correlation (right) for northward and eastward convection velocities as a function of $(V_{sw}/500)^2 B_z$, (V_{SW} is the solar wind flow speed, in km s^{-1}, B_z the northward component of the IMF in nT and GSM co-ordinates). Negative lags are defined as the interplanetary medium leading the ionospheric flows. The data were taken at 3 invariant latitudes (Λ = 70.8°, 72.0° and 73.4°, for gates 1,3 and 5, respectively) on 5 days of simultaneous EISCAT-AMPTE observations, with the MLT of the radar field-of-view in the range 13:00 - 15:00. Results for eastward (northward) flow are shown by solid (dashed) lines on the left and by crosses (squares) on the right (after /13/).

The ionospheric response times, T_{MR}, deduced from the cross-correlations, are shown in figure 4 as open circles (joined by a dotted line) as a function of the MLT of the centre of the radar field-of-view (R). A consistent trend is seen in the data, with the lowest response times in the early afternoon sector and larger values nearer dawn and dusk. A study of the effect of beamswinging for various onset times of step-function increases in flow speed has shown that this technique increases rise times but is very unlikely to alter the ionospheric response time deduced /14/.

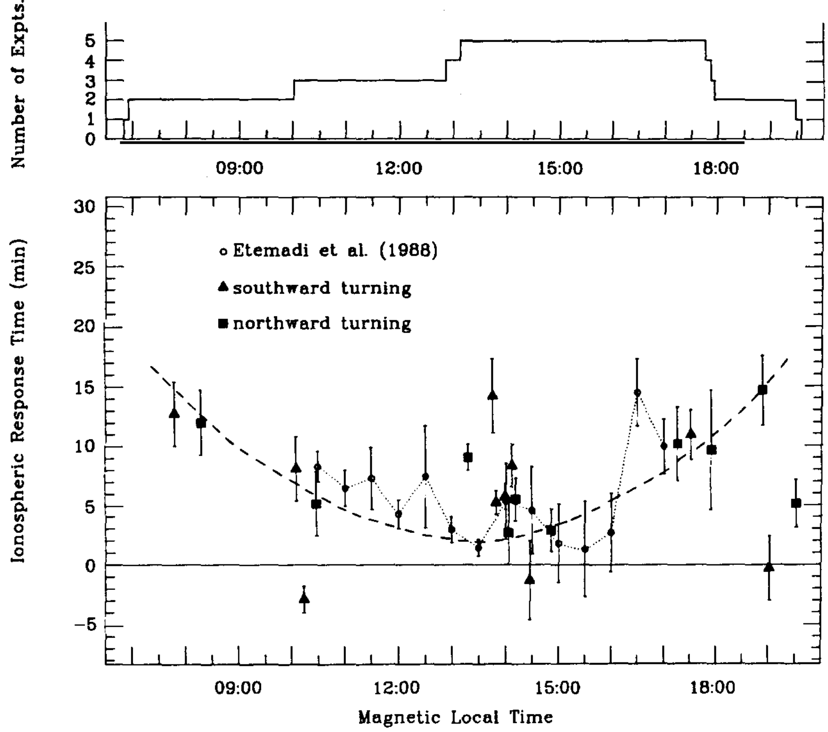

Fig. 4. Number of combined EISCAT-AMPTE experiments (top) and deduced ionospheric response time, T_{MR}, (bottom) as a function of MLT of the radar field-of-view (R). Open circles show the results for the statistical survey of 2.5-minute vector data /13/ and triangles and squares are case studies of individual southward and northward turnings, respectively, using 15-second line-of-sight velocities /12/. The dashed line is the predicted curve from the model of Lockwood et al. /11/ for $\Delta\Phi_m$ = 100 kV.

These results concerning response time have been verified using a completely different approach to the same EISCAT-AMPTE dataset. This employs the 15-second line-of-sight velocities, V_{los}, without deriving vectors by the beamswinging technique. A survey of the 15-second 'Polar' data has been presented by Todd et. al. /15/ and here we adopt their data presentation format. Examples of 15-second data are given in figures 5 and 11: the V_{los} observed for the easterly look-direction are denoted by triangles; those for the westerly look-direction by squares, and those taken while the antenna is in motion between the two by inverted-Y symbols. For constant, uniform flow across the radar field-of-view, the beamswinging places a "square-wave" modulation on the V_{los} values: the amplitude of this square wave is proportional to the zonal, magnetically east-west component of the flow, and the mean value is proportional to the northward component of the flow. Figure 5 (a) and (b) are two examples (from references /15/ and /12/, respectively) of observations with R in the centre of the auroral flow "channel", where flows are largest and relatively smooth /15/. The lower 4 panels give the V_{los} values for the first 4 range gates (corresponding to the invariant latitudes given to the right of the figure. The top panels show the B_z component of the IMF observed by AMPTE-UKS. The bottom UT scale applies to the EISCAT data, the top one to the AMPTE data and the two have been offset by the predicted satellite-to-magnetopause propagation delay, T_{SM}. It can be seen that figure 5a shows another example of a southward turning of the IMF, while 5b contains a northward turning some 20 minutes later (these events are at MLT of 14:30 and 14:50, respectively). The EISCAT data show a smooth variation in response, with great consistency from one 15-second V_{los} value to the next. In figure 5a, the afternoon-sector westward flows are seen to begin to increase (from the amplitude of the "square wave") after a delay of only a few minutes and to evolve over a period of about 5 minutes. Similarly, in Figure 5b, the flows begin to respond to the northward turning after an ionospheric response time of just a few minutes and have a characteristic decay time of order 5 minutes. In both cases, the flow for northward IMF is a factor of 3 slower than that for southward IMF. For long periods of northward IMF, there is a more gradual decay of the residual flow speed /12/.

The onsets of the ionospheric responses to the events shown in parts (a) and (b) of figure 5, and to the other 9 southward and 9 northward sudden turnings of the IMF during the EISCAT-AMPTE observations, were timed using the 15-second V_{los} data: the results are shown by the triangles and squares, respectively, in figure 4. It can be seen that the general trend of the statistical survey is followed by these events, although there is considerable scatter. Some of the reasons for this are discussed in the following section.

The response times for dayside convection are consistent with several sets of previous observations. As long ago as 1968, Nishida /45/ reported that the DP2 current system correlated with IMF B_z with lags of only 5-10 minutes and Reiff et al. /46/ have found the cross-cap potential derived from a global magnetometer network by the 'KRM' method shows a similar response. Holzer et al. /17/ deduced that polar cap area (defined from precipitation boundaries) began to increase after a similar delay following a southward turning of B_z. Clauer and Fris-Christensen /47/ have shown that the rotation of polar cap flows to sunward began after an even shorter delay (only an Alfvén wave transit time) following a northward turning of B_z; however, the flows then evolved over a longer period (20 minutes) than for the auroral flows discussed here.

The colour plot of the bottom panel in figure 2 shows an ion temperature enhancement following the southward turning of the IMF, due to enhanced ion-neutral frictional heating. Such ion temperature changes are very useful markers of flow variations, either purely temporal (as in figure 2) or due to moving spatial features (as in figure 9).

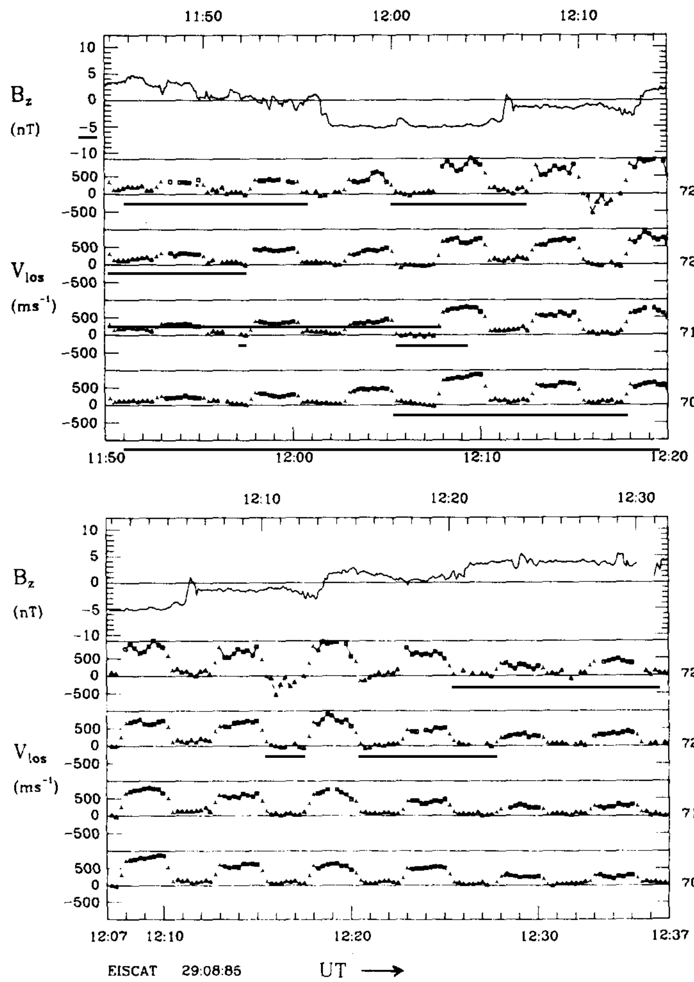

Fig. 5. Examples of southward (top) and northward (bottom) turning events both from 29 August, 1985. In each plot, the top panel gives the IMF B_z component and the lower 4 panels the 15-second line-of-sight flow velocity (for the invariant latitudes given to the right of the figure). Squares are values from geographic azimuth (east of north) 332°, triangles from 356°. The IMF and flow data have been offset by the predicted propagation delay, T_{SM}, and the top (bottom) UT scale refers to the IMF (convection) data, respectively (after /12/ and /15/).

Figure 6(a) shows 30-second integrations of the ion temperatures for this period for one range gate. It can be seen that the ion temperature rise for the more westerly look direction (azimuth 1) leads that for azimuth 2. Figure 6(b) shows a cross-correlation analysis of the T_i sequences seen at the two azimuths, and reveals that peak, and most significant, correlation is for a lag of 2.0 ± 0.25 min /11/. This gives an eastward propagation of the ion temperature and flow speed enhancements of 2.6 ± 0.5 km s^{-1}. The same eastward speed was found for all range gates, but no lag was detected between the variations at different latitudes, hence the convection equipotentials were deduced to be moving almost purely eastward around the afternoon sector auroral oval, away from noon.

THE EXCITATION OF IONOSPHERIC CONVECTION

The observation that ionospheric flows respond rapidly to both southward and northward turnings of the IMF is not consistent with the concept that all open field lines impart momentum to the ionosphere. The evidence for a residual effect, attributed to the field lines which remain open following a northward turning continuing to impart momentum to the ionosphere, comes from studies of cross-cap potential /16/. If this were the case, the polar cap is a sufficiently large resevoir of open field lines that the time constant for growth and decay of cross-cap potential, and of the convection pattern as a whole, should be that of the polar cap area, i.e. several hours (as observed from precipitation boundaries /17/ and global auroral images /18/).

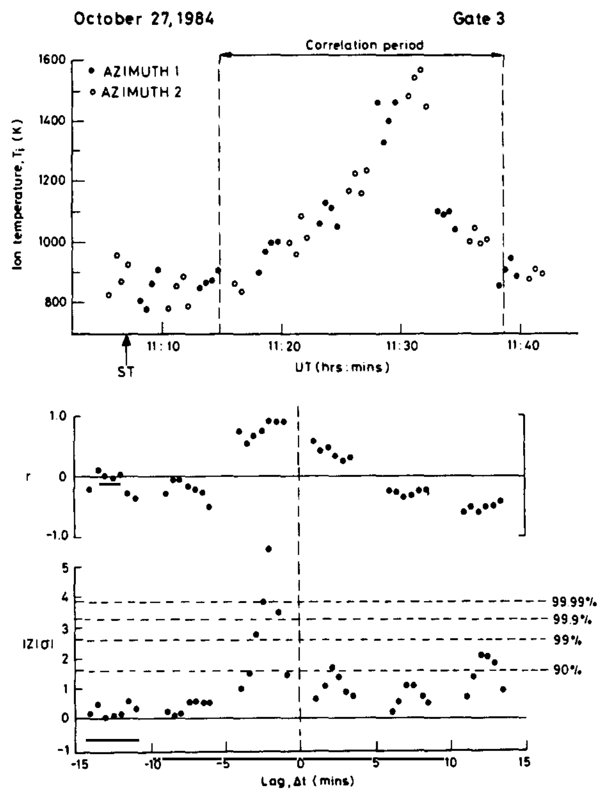

Fig. 6(a) Ion temperatures observed at 30-second resolution at azimuth 1 (332° - open circles) for the period around the first flow enhancement shown in fig. 2. (b). cross-correlation coefficient ,r, and Fisher-Z significance parameter, as a function of lag, for the data sequences shown in (a). Negative lags correspond to azimuth 332° leading, i.e. an eastward propagating temperature enhancement (after /11/).

The data presented in the previous section are consistant with the schematic shown in figure 7, taken from Lockwood and Freeman /19/. This is an adaptation of the work by Siscoe and Huang /20/ who showed that a two-celled convection pattern would be driven in the ionosphere if reconnection allows flux to enter the polar cap on the dayside, even if there is no reconnection in the tail to give flow out of the polar cap. Under such circumstances the cap must expand, according the Faraday's Law. Siscoe and Huang considered the merging gap (the ionospheric projection of the magnetopause neutral line) to remain stationary, in which case the return auroral flows are 'driven' in the ionosphere by the expansion of the "adiaroic" (meaning "not flowing across") polar cap

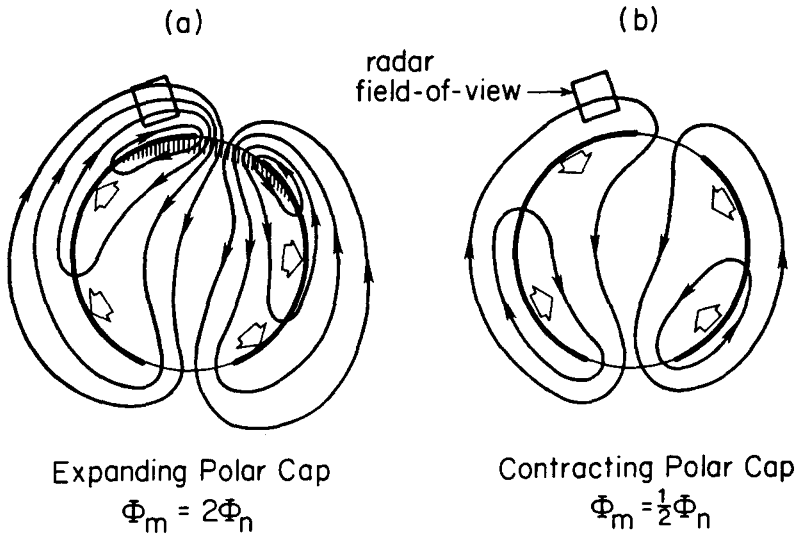

Fig. 7. Schematics of convection patterns for uniformly expanding (a) and contracting (b) polar caps (after /19/).

boundaries. (The virtually incompressible nature of the ionosphere allows such simple hydrodynamic concepts to be employed). In figure 7, a constant potential of Φ_n exists across the tail neutral line, compared with Φ_m across the magnetopause neutral line. Figure 7(a) shows the case for $\Phi_m = 2\ \Phi_n$, for which the sunward flow of auroral closed field lines is half driven by the reconnection in the tail and half by the equatorward expansion of the polar cap. In part (b), we simulate the convection pattern immediately following a northward turning of the IMF by reducing Φ_m by a factor of 4. We consider Φ_n to remain constant as a change in the IMF has not yet affected the tail neutral line: correlative studies of the DP 1 current system indicate that Φ_n only reacts to a change in B_z after a lag of greater than 0.5hr. In Figure 7(b), the poleward moving adiaroic boundaries of the resulting contracting polar cap ($\Phi = 0.5\ \Phi_n$) effectively detract from the auroral flow driven by the release of tail stress by reconnection. Note that the centres of the convection cells move antisunward from near the ends of the dayside merging gap to nearer the ends of the projection of the tail neutral line. Figure 7 predicts that convection strength in the dayside auroral zone is modulated by the rate of change of cap area, rather than the magnitude of the area, giving the observed responses on time scales of a few minutes and not hours.

To be consistent with Figure 7, flows in the dayside polar cap must decay on time scales of a few minutes. Figure 8 is an example of 'Polar' data showing precisely this behaviour. The 2.5-minute flow vectors show very strong, westward afternoon cell convection in all range gates for the period 09:00 - 11:25 UT (≈ 11:35 - 14:00 MLT), when the IMP-8 satellite observes the IMF to be predominantly strongly southward. Starting at 11:25 UT, the polar cap boundary expands across the field of view in about 15 minutes, this change seemingly being due to a reversal in polarity of B_y, from positive to negative and a return to strong southward B_z after a northward excursion of duration 3 min. At 11:40 UT a rapid decay of polar cap flow commences at all latitudes. The decay taking some 10 minutes near $\Lambda = 72°$, but only 5 minutes at $\Lambda = 74°$. The flow becomes weakly northward, the convection speeds being equal to the poleward speed of the boundary as it contracts back across the first two range gates. This is as predicted by figure 7. Note that the polar cap flow has decayed, the boundary has not rapidly contracted: the boundary does not return to range gate 7 until 13 UT. The auroral zone flow channel which contracts back across the field of view between 13:00 and 13:30 UT is remarkably weak compared to the flows seen before the decay at 11:40 UT. Because of a gap in the interplanetary magnetic field data, it is not known if the decay is caused by a northward turning of B_z (affecting both convection cells), or a polarity reversal of B_y (causing the dawn cell to grow at the expense of the dusk cell). However, the cause is not as important to this paper as the fact that polar cap flows are seen to diminish on the same short time scales (5-10 min), as was inferred from the auroral zone measurements. This means that open field lines only impart significant momentum to the ionosphere for a relatively short period of time (5-10 minutes) compared with the cross-cap transit time (typically 1 hour). From these data, Lockwood et. al. /21/ deduce that significant momentum is transferred into the ionosphere only in the crescent-shaped region shaded in figure 7(a) and that this region is only a few degrees of invariant wide and about 6-8 hours of MLT in length.

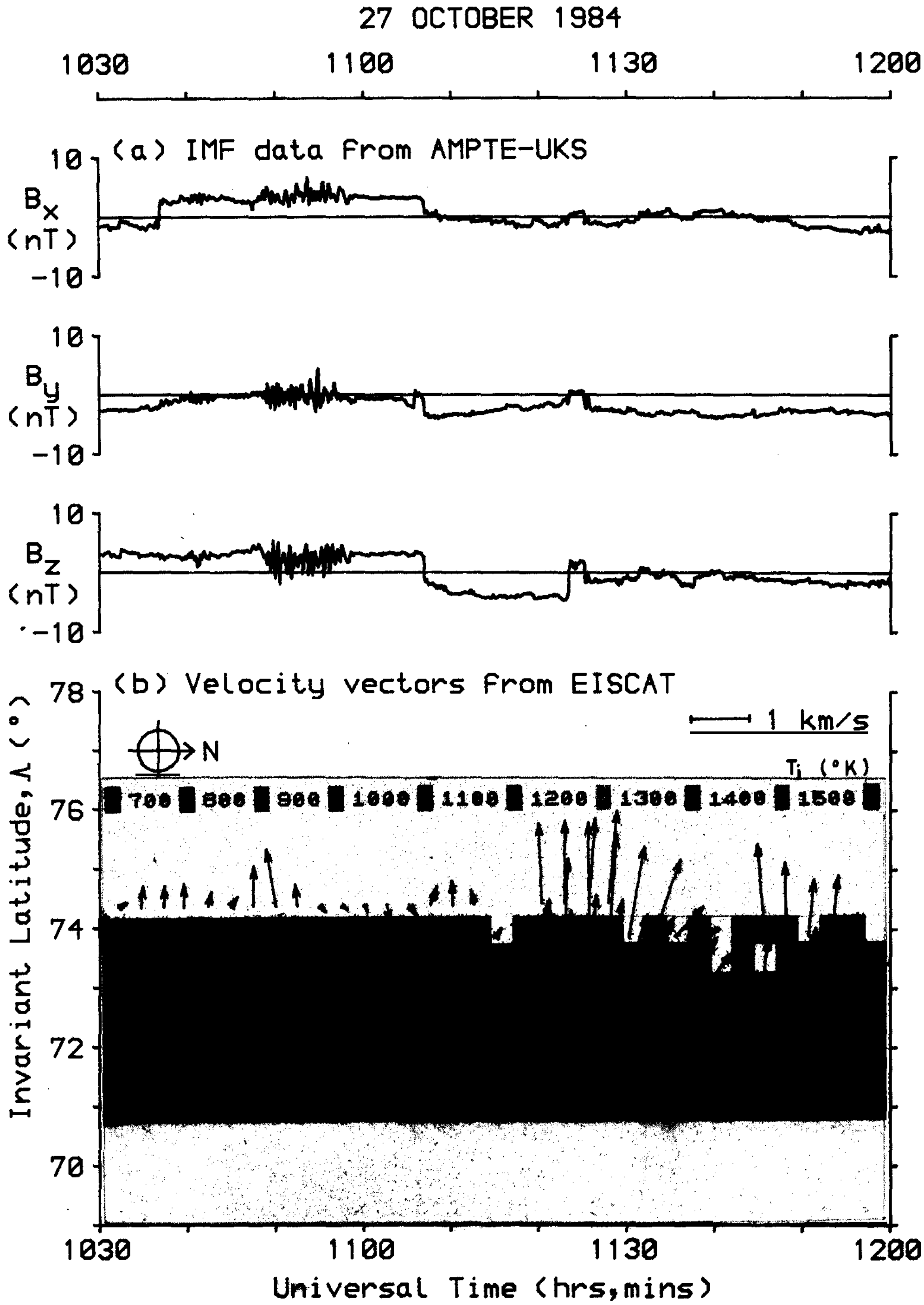

Fig. 2. An example of simultaneous observations of (a) the IMF by AMPTE-UKS (in GSM co-ordinates) and (b) the ionospheric flows and ion temperatures observed by EISCAT on 27 October, 1984. The 2.5-minute resolution EISCAT convection data are shown in "electric field" format with westward flow denoted by vectors pointing up the page, and are superposed on 2-minute averages of ion temperature, T_i. Strong enhancements in flow speed and T_i are seen 11 minutes after the abrupt southward turning of the IMF at 11:07 UT, and 21 minutes after the much weaker event at 11:25 UT /9,10,11,/.

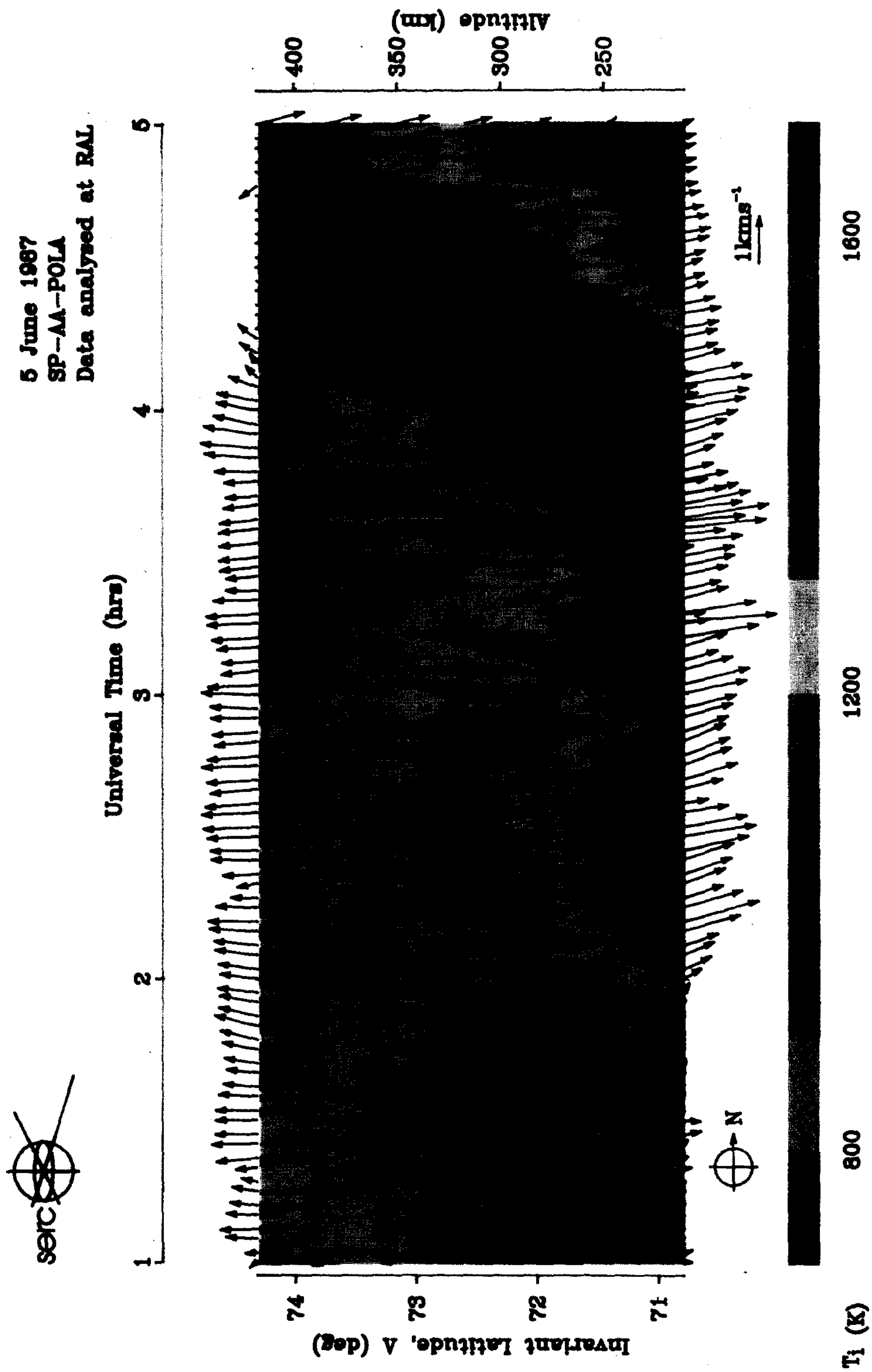

Fig. 9. EISCAT vector flow and ion temperature data from the 'polar' experiment on 5 June 1987, showing viscous interaction across a contracting polar cap boundary (see text). the data presentation format is as used in the bottom panel of fig. 2 (after /26/).

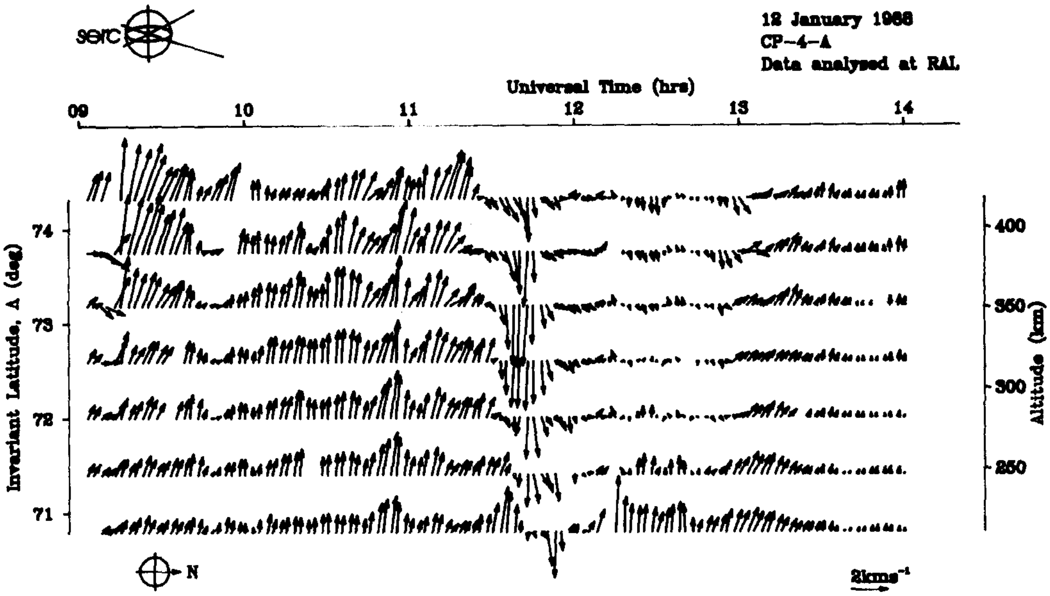

Fig. 8. EISCAT vector flow data from the CP-4 experiment (effectively identical to 'Polar') on 12 January 1988, showing rapid decay of polar cap flows near 11:40 UT. The data presentation format is as used in the bottom panel of fig.2 (after /21/).

The feet of flux tubes poleward of this crescent-shaped region do, of course, move antisunward, at least when the IMF is southward, but they are pushed by more newly-reconnected flux tubes. The magnetopause ends of all open flux tubes are still moving tailward with the solar wind speed, but after they have reached a few tens of Earth radii tailward of the Earth little further effect will be produced in the near-Earth magnetic field and little or no momentum will be transferred down into most of the polar cap ionosphere.

This concept is also consistent with the picture of a new, expanding convection pattern following a southward turning proposed by Lockwood et al. /11/. The only unresolved question concerning the explanation of figures 2 and 6, as put forward by these authors, was why the convection pattern associated with the region of newly-opened flux was so very much more vigorous than that for the entire "old" polar cap. This problem is resolved by the fact that only the newly-opened flux tubes impart significant momentum to the ionosphere. If we assume that the dimensions of the region always have the ratio of latitudinal width to longitudinal extent of 6 /21/ then a 100 kV increase in Φ gives a response time variation with MLT, predicted using the Lockwood et al. /11/ model, shown by the dashed line in figure 4. It can be seen that this curve is close to the average of the observed values: the scatter is to be expected if there is a variety of MLT of the ionospheric onset and/or of $\Delta\Phi_m$. The minimum T_{MR} may be explained by any time for flux tubes to straighten before they impart momentum to the ionosphere /22, 19/ and/or a lag T_{CR} due to R being equatorward of C (see fig.1). Furthermore, the deduced T_{CR} (the observed T_{MR} minus the Alfvèn wave propagation time to the ionosphere) for the major event shown in figures 2 and 6 yields an expansion speed of 2-3 km s^{-1}, for the above values of $\Delta\Phi_m$ (which is consistent with the observed IMF and solar wind using the regressions of Φ discussed in references /5,6,7 and 46/), compared with an observed value of 2.6 km s^{-1} /11/.

Other anomalous details of figure 2 are explained by the proposed mechanism for excitation of ionospheric convection. For example, the IMF returned northward at 11:23 UT and the ionospheric flows begin to slow 7 minutes later (after the last reconnected flux tube had straightened and begun to impart momentum to the ionosphere, calling for a straightening time of some 2 minutes). The flows then decrease by a factor of 3 in the next 5 minutes (implying the last reconnection flux tube imparts most of its momentum in 5 minutes). The enhancement in flows following the second, minor, southward turning at 11:25 UT does not reach the radar field of view until 11:46 UT and is much more gradual, calling for a $\Delta\Phi_m$ of only 40 kV (which is also consistant with the observed IMF and solar wind) for the "spreading smile" model proposed by Lockwood et al. /11/.

Lastly, we note that this model allows covection to vary in response to short time-scale variations in polar cap area, shorter than those observed in multi-radar studies of large-scale expansions and contractions of the convection reversal boundary /23,24,25/.

OBSERVATIONS OF VISCOUS-LIKE INTERACTION

The primary evidence for some form of "viscous-like" interaction at the magnetopause is the residual cross-cap potential, driving net antisunward flow, observed when the IMF is northward /5,6,7/. The analysis presented in the previous section does not allow as much of this potential to be attributed to the effect of residual open field lines as had previously been thought, although there will be residual Φ_n due to tail reconnection, as energy stored in the geomagnetic tail is released. In this section, because there are no multipoint observations of the viscous-like interaction to report, we suggest some which should be attempted in the light of recent ionospheric measurements.

Figure 9 shows a 5-hour sequence of EISCAT 'Polar' flow data in the same format as used in figures 2 and 8. The plot shows the convection boundary contracting poleward across the field-of-view between 2:00 and 4:15 UT (roughly 4:30 - 6:45 MLT). The colour ion temperature contours show a strong enhancement equatorward of the contracting boundary, with an almost step-function rise at the reversal. The ion temperatures at the 2 azimuths have been used by Lockwood et al. /26/ to define the orientation of the boundary and hence to show that the boundary is not quite adiaroic, i.e. that this is not quite a perfect velocity shear moving across the radar field of view. More specifically, the speed of poleward convection normal to the boundary, consistantly exceeds the poleward contraction speed of the boundary, by an amount which is much larger than the maximum error introduced by the beamswinging technique employed. Hence field lines are either being opened at this pre-dawn MLT, or this boundary maps to the flanks of the magnetotail where viscous-like interaction takes place, in the manner suggested by Heikkila /28,29/ or more specifically by Richardson et al. /27/. The potential across the 2-hour segment of boundary observed is 7±1 kV. Hence between one third and half of the cap boundary would have to be subject to an interaction of this rate of momentum transfer to explain the residual cross-cap potential for northward IMF /5,6,7/. That these potentials are somewhat larger than those deduced across the near-Earth boundary layer /28,30,31/, indicates that the viscous-like interaction may take place mainly in the far magnetotail /28/. It is also evident that there is a slowing of the flow at the boundary in figure 9, which may well signify that the potential at the magnetopause exceeds these values seen in the ionosphere, the difference being "shorted-out" from the ionosphere by inverted-V structures /32/.

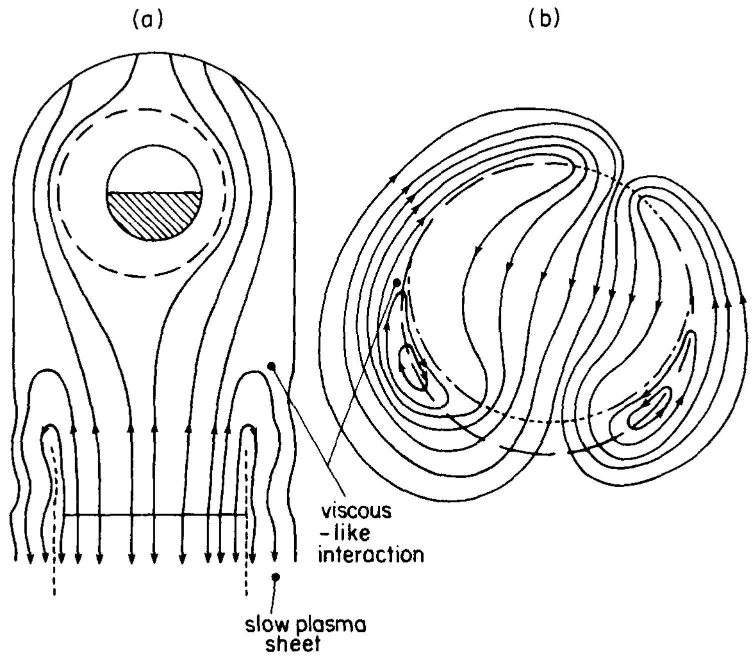

Fig. 10. Schematic illustration of viscous-like interaction: flow snaphots in (a) the equatorial plane (after /27/) and (b) the polar ionosphere (after /26/).

Figure 10(a) is a schematic of the equatorial magnetospheric flow during low magnetic activity deduced by Richardson et al. /27/ from analysis of ISEE-3 data in the far tail from the CDAW-8 analysis periods. Figure 10(b) shows the consistent ionospheric flows observed by Lockwood et al. /26/: note that the accumulation of closed field lines in the tail (and poleward of the convection reversal in the ionosphere) is envisaged to be lost in sudden 'pinching-off' events /26/. In both datasets, there are indications that the momentum transfer is associated with Kelvin-Helmholtz waves. Hence it is possible that the potential is not a constant base-level, but increases during quiet periods when the length of the Kelvin-Helmholtz unstable tail is increased. These observations call for simultaneous multipoint measurements to be made on the flanks of the tail and at the nightside ionospheric convection boundary to investigate these ideas.

OBSERVATIONS OF EFFECTS OF TRANSIENT RECONNECTION

The observations by Goertz et al. /3/, discussed in the introduction, remain the only multipoint observations which indicate a flux transfer event both in the ionosphere and at the magnetopause. Figure 11 shows a "flow burst" event, of a kind seen regularly but relatively infrequently in the dayside auroral oval using the 'Polar' experiment /15/,

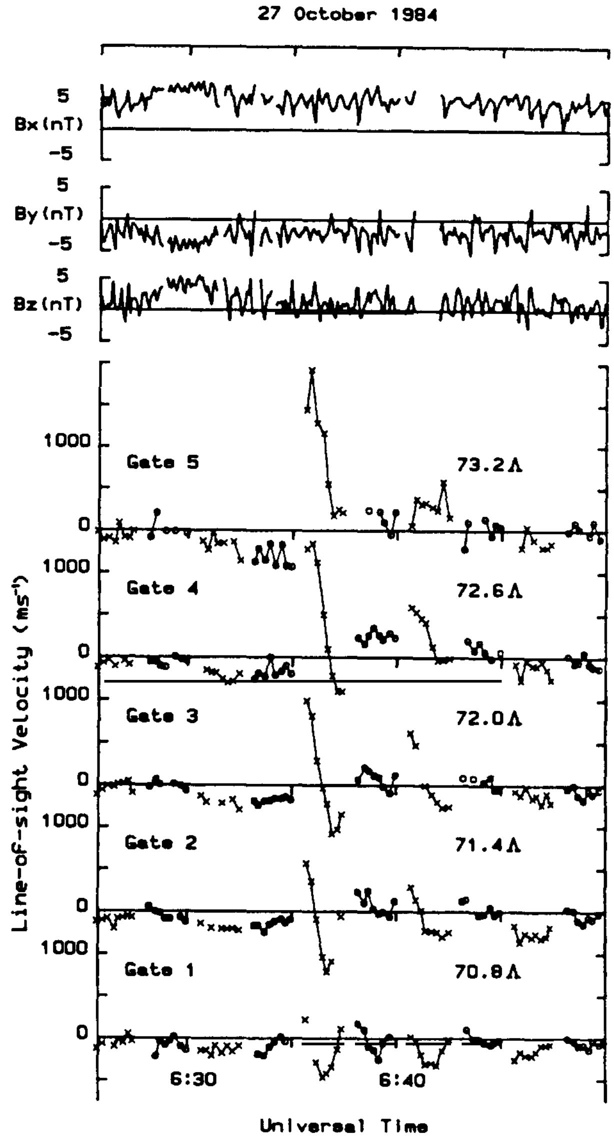

Fig. 11. EISCAT 15-second flow data from the 'Polar' experiment on 27 October 1984, showing an impulsive flow-burst event in the dayside auroral ionosphere, with AMPTE-UKS observations of the IMF. The data presentation format is that used in fig. 5 (after /33/).

which Todd et al. /33/ have shown to be consistent with the Southwood /22/ model of the ionospheric signature of an FTE and which Kokubun et al. have also identified in magnetometer data /50/. The IMF data from AMPTE-UKS show no clear trigger for this event, but neither is there any detectable change in the high time-resolution dynamic pressure data. However, co-ordinated observations on about 10 days using 'Polar' with the ISEE satellites at the dayside magnetopause have failed to show any events for which a flow burst could be associated with an FTE (R.C. Elphic, private communication). In this section, we therefore discuss why multipoint detection of FTEs is so elusive and why flow burst events are much less common than magnetopause FTEs.

Figure 12 is a schematic of two extreme cases of FTE evolution. In (a) the join of magnetosperic and magnetosheath arms of the reconnected tube moves directly antisunward whereas in (b) it moves towards dawn or dusk at low latitudes. The motion for any one FTE will depend on the dominance of sheath flow over magnetic tension or visa-versa. From the discussion section on the excitation of ionospheric flows, we can deduce that the FTE will impart momentum to the ionosphere for up to 10 minutes, if it moves around the cap boundary (as in fig 12b), but for only 2-3 minutes if it moves poleward into the polar cap (as in 12a). There will only be an ionospheric signature of an FTE while it is moving faster than the surrounding flux tubes and hence we should expect lifetimes of just 2-10 minutes in the ionosphere. In the case of a poleward-moving signature, this means an FTE may only move about 100km, roughly its own spatial dimension. Hence there is a great difference between the probabilities of an FTE being dragged poleward over a magnetopause spacecraft (figure 11a) and of the ionospheric signature of an FTE forming and then decaying within the field of view of an ionospheric observatory. None-the-less recent observations of putative ionospheric ions in the wake of an FTE, of the type descrlbred schematically in fig. 12b /34/, indicate that some simultaneous observations of such FTEs should be possible, albeit rarely.

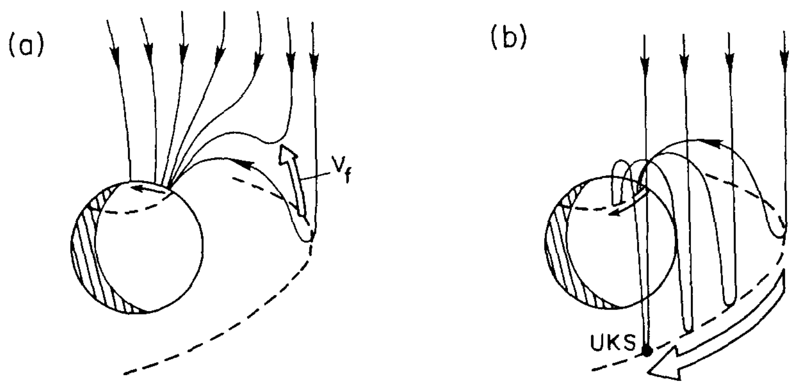

Fig. 12. Schematics of extreme cases of evolution of newly-opened flux tubes.

A major unresolved question concerning FTEs is how much potential is associated with each event. The values often quoted assume that the newly-opened flux tube is circular in cross section, i.e. the Russell and Elphic model /4/. However, only the dimension in the direction of motion of the tube is accurately known and recent theoretical work indicates that the perpendicular dimension could be considerably greater /35/, increasing the FTE potential estimate by the major to minor axis dimension ratio. Ground-based radars are the best way to determine this axis ratio and hence the potential. However, very few radar systems can observe plasma flows across the dayside convection reversal with the sub-minute resolution required to detect FTEs. Those that can tend to be too far equatorward, like EISCAT (even in 'Polar' mode) and STARE, for the dayside convection boundary to be within the field of view on any more than a small fraction of days. Ironically, others are too close to the region of interest: Sondrestrom, for example, frequently views the cleft along the magnetic field line and has to employ latitude scans with severe penalties for temporal resolution. Coherent systems have the required spatial coverage and temporal resolution but also have difficulties in providing the necessary continuous monitor of the convection boundary, due to periods without scattering irregularities. We believe the requirement for a radar to continuously monitor convection in the cleft region with high time resolution is very urgent, particularly in view of the forthcoming CLUSTER mission.

Optical photometers, which scan the meridian with very high temporal resolution, have shown many of the features which we expect for ionospheric signatures of FTEs /36,38,50/. In addition to showing 5-8 minute repetition periods, systematic behaviour with IMF B_z and B_y, and election precipitation of much greater energies than the usual cleft aurora (all consistent with FTEs), the motions (see /34/) and lifetimes (2-10 min) of the observed events are as predicted here for FTEs. Combined observations with all-sky cameras allow the longitudinal extent of the events to be studied. An example of such a case has yielded a potential of 50 kV /36/. Lastly, events have been reported which are consistent with the predicted signature of FTEs in data from ground-based magnetometers /e.g. 37,38,50/. In the following section, we show care must be taken when analysing such events, because similar effects will be produced (albeit over a greater range of locations) by dynamic pressure changes. Consequently, unambiguous detection of FTEs requires a close-packed array (<500 km extent) of high-time resolution magnetometers /39/ and a wider array of stations to eliminate the effects of dynamic pressure changes. Supporting information from other instruments (for example photometers /36/, all-sky cameras /38/ or radars /50/) aids the identification of an event as an FTE.

EFFECTS OF DYNAMIC PRESSURE CHANGES

Dayside magnetometer chains have shown large scale signatures consistent with one, two or continuous trains of travelling convection vortices /40,41,42/. The events are several thousand kilometres in extent, considerably larger than expected for FTE signatures, and move at great speeds (4-6 km s^{-1}), tailward around the convection boundary. In addition, the flow at the centre of the event is not the same as the motion of the event as a whole, as is required for a FTE /22/. Friis-Christensen et al. /41/ have shown that one particular twin-vortex event is associated with either a dynamic pressure change or a change in the location of reconnection (due to a change in polarity of B_y). A notable set of multipoint measurements, comprising data from IMP-8, AMPTE-CCE, VIKING and ground magnetometers has been presented for two similar events by Potemra et al. /43/. Although these data identify toroidal standing Alfvèn waves and strongly imply a ringing and a driven response to, respectively, step function and periodic variations in dynamic pressure, there are accompanying changes in both IMF B_y and B_z, and hence reconnection variations cannot be completely ruled out.

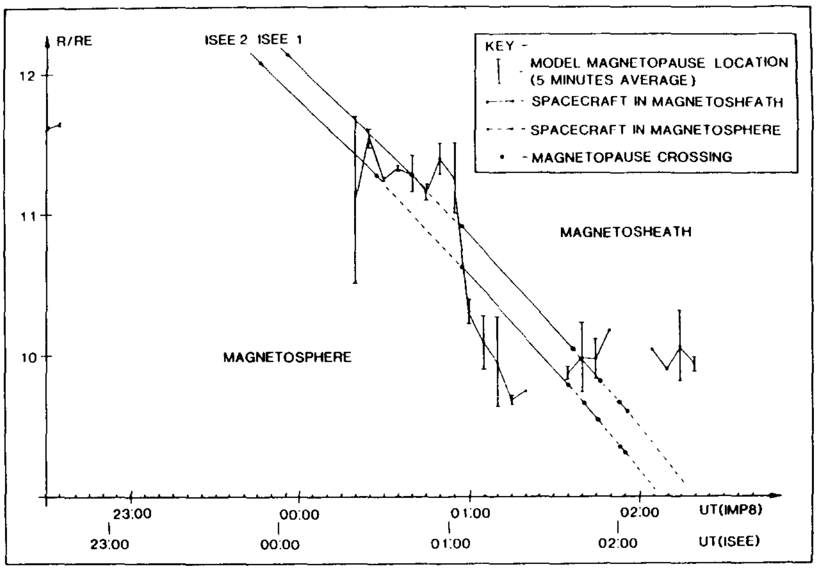

Fig. 13. Predicted and observed magnetopause locations from IMP-8 dynamic pressure observations and ISEE-1 and -2 particle and magnetic field observations, respectively, on 10 September, 1978 (after Farrugia et al. /44/).

Figures 13 and 14 describe an example of one of these events which is unambiguously triggered by a compression of the magnetopause (from Farrugia et al. /44/). During this period, the IMF was steady and purely northward (i.e. $B_z \simeq B$), which eliminates any possiblity of an effect of reconnection at the subsolar magnetopause. Figure 13 shows inbound passes of ISEE-1 and -2, in a radial distance, R, - UT frame : solid orbit portions are where the spacecraft is identified by plasma and magnetic field observations to be in the magnetosheath, dashed portion are within the magnetosphere. At about 00:18 UT and 00:33 UT, ISEE-2 and then ISEE-1, crossed into the magnetosphere. Because in both cases the magnetopause was near $R = 11.3R_E$, this is an equilibrium position for the steady solar wind (speed and density) observed by IMP-8 prior to 00:55 UT. Between 00:55 and 01:10 UT the solar wind dynamic pressure was seen to rise dramatically, principally due to an increase in density. The curve in figure 13 is the predicted magnetopause location from the 5-minute averages of the observed solar wind dynamic pressure, computed from the observed equilibrium position and with predicted propagation delay, T_{SM}, of about 7.5 min. It can be seen that predicted and observed magnetopause locations agree very closely, confirming that the rapid inward motion seen by ISEE-1 and -2 near 01:05 UT is a compression due to dynamic pressure increase, commencing close to 01:02 UT. Figure 14 shows the magnetograms observed at two stations in the Alaskan chain: in both cases, all 3 components showed little variation for extended periods around that shown, (which commences at 01:00 UT). It can be seen a major bi-polar signature in the X component is observed to commence near 01:04 UT at both stations, i.e. roughly one Alfvén wave magnetopause-to-ionosphere transit time (T_{MC}) after the onset of the compression event.

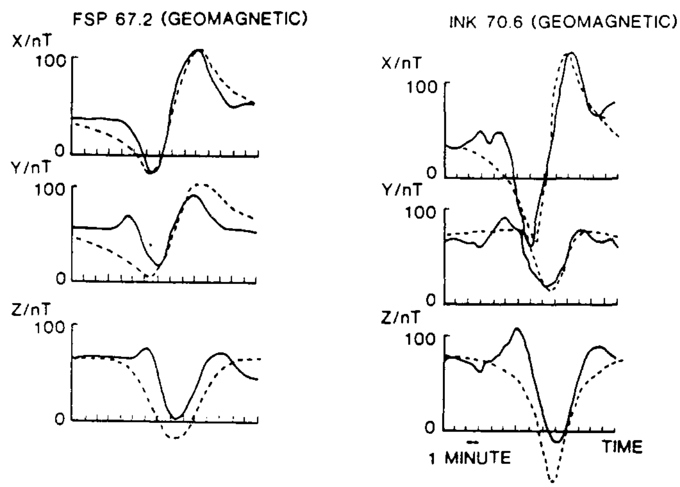

Fig. 14. Magnetometer recordings at 2 northern hemisphere, auroral observations, commencing at 01:00 UT on 10 September, 1978, showing the effects of the dynamic pressure increase and magnetopause compression presented in fig. 13. The dashed lines are FTE predictions (from /44/).

In order to illustrate how closely this effect can mimic an FTE at one magnetometer station, the dashed lines plotted in figure 14 show fitted predictions for FTE models. In fact, different models have been used in each case, from the work of McHenry and Clauer /39/. Either model gives a satisfactory fit to an event which is known not to be an FTE. This could, however, have been recognised from ground-based data alone as the event was seen at over a 12° range of latitudes (making the event at least 5 times longer in that dimension than expected for an FTE) and at over more than 3 hours of MLT (only consistent with the Southwood et al. /35/ FTE model). In addition, the event propagated at 6 km s^{-1} (a very large speed for an FTE) and resonant ringing was observed at its centre (at 68.1° geographic latitude, i.e. between the stations shown in figure 14), which is not expected for an FTE.

CONCLUSIONS

The value of ionospheric observations to studies of momentum transfer from the solar wind is now evident. Studies of dayside convection have shown the direct control to be exerted by the B_z component of the IMF. The rapid response to both southward and northward turnings of the IMF indicate that significant momentum is transferred from the solar wind into the ionosphere only in the region immediately poleward of the cusp, by newly-opened flux tubes. The pattern driven by this momemtum transfer is the convection equivalent of the DP2 current system and will be superposed on that driven in the nightside ionosphere by release of tail stress (equivalent to the DP1 system).

The dayside pattern is observed to expand rapidly (at speeds which exceed convection velocities) following a southward turning of the IMF, as the region of momentum transfer is filled with newly-opened flux tubes.

These findings also indicate that FTE signatures in the ionosphere should be short-lived (2-10 minutes) and will only move over a short distance (100-600 km). This explains the low occurence frequency of putative FTE signatures in the ionosphere, relative to that at the magnetopause. In addition, care must be taken when searching for FTEs with ground-based instrumentation, to eliminate the effects of any dynamic pressure changes which can mimick FTE effects, at least for an isolated observatory. However, the impulsive flow bursts in the dayside auroral oval observed by EISCAT are certainly not due to dynamic pressure changes in the solar wind.

Ground-based radar has also revealed nightside flows across the convection boundary, into the polar-cap, which are seemingly consistent with a viscous-like interaction on the flanks of the magnetotail.

Acknowledgements. We thank D.J. Southwood, H. Lühr and D.R. Lepping for AMPTE-UKS, -IRM and IMP-8 magnetometer data respectively and the director and staff of EISCAT for their assistance. EISCAT is supported by the research councils of France (CNRS), West Germany (MPG), Norway (NAVF), Sweden (NFR), Finland (SA) and the UK (SERC). We are grateful to D.J. Southwood, M.P. Freeman, C.J. Farrugia and H. Todd for scientific discussion, S.R. Crothers for graphics, and K.S.C. Freeman for processing the EISCAT CP-4 data.

REFERENCES

1. G. Paschmann, I. Papamastorakis, W. Baumjohann, N. Sckopke, C.W. Carlson, B.U.O, Sonnerup and H. Lühr, The magnetopause for large magnetic shear: AMPTE/IRM observations, J. Geophys. Res., 91, 11099 (1986)

2. M.P. Freeman and D.J. Southwood, The effects of magnetospheric erosion on mid and high latitude ionospheric flows, Planet. Space Sci., 36, 509 (1988)

3. C.K. Goertz, E. Nielsen, A. Korth, K.-H. Glassmeier, C. Haldoupis, P. Hoeg, and D. Hayward, Observations of a possible ground signature of flux transfer events, J. Geophys. Res., 90, 4069 (1985)

4. C.T. Russell and R.C. Elphic, Initial ISEE magnetometer results: magnetopause observations, Space Sci. Rev., 22, 681 (1978)

5. S.W.H. Cowley, Solar wind control of magnetospheric convection, in: Achievements of the International Magnetospheric Study IMS, ESA SP-217, ESTEC, Noordwijk, the Netherlands, p. 483-494 (1984)

6. S.W.H. Cowley, The impact of recent observations on theoretical understanding of solar wind-magnetosphere interactions, J. Geomag. Geoelectr., 38, 1223 (1986)

7. P.H. Reiff, and J.G. Luhmann, Solar-wind control of the polar-cap voltage, in: Solar Wind-Magnetosphere coupling, ed. Y. Kamide and J.A. Slavin, Terra Scientifica, Tokyo, p. 453-476 (1986)

8. A.P. van Eyken, H. Rishbeth, D.M. Willis and S.W.H. Cowley, Initial observations of plasma convection at invariant latitudes 70-77°, J. Atmos. Terr. Phys., 46, 635 (1984)

9. D.M. Willis, M. Lockwood, S.W.H. Cowley, A.P. van Eyken, B.J.I. Bromage, H. Rishbeth, P.R. Smith and S.R. Crothers, A survey of simultaneous observations of the high-latitude ionosphere and Interplanetary Magnetic Field with EISCAT and AMPTE-UKS, J. Atmos. Terr. Phys., 48, 987 (1986)

10. H. Rishbeth, P.R. Smith, S.W.H. Cowley, D.M. Willis, A.P. van Eyken, B.J.I. Bromage and S.R. Crothers, Ionospheric response to changes in the interplanetary magnetic field observed by EISCAT and AMPTE-UKS, Nature, 318, 451 (1985)

11. M. Lockwood, A.P. van Eyken, B.J.I. Bromage, D.M. Willis and S.W.H. Cowley, Eastward propagation of a plasma convection enhancement following a southward turning of the interplanetary magnetic field, Geophys. Res. Lett., 13, 72 (1986)

12. H. Todd, S.W.H. Cowley, M. Lockwood, D.M. Willis and H. Lühr, Response time of the high-latitude dayside ionosphere to sudden changes in the north - south component of the IMF, Planet. Space Sci., in press, (1986)

13. A. Etemadi, S.W.H. Cowley, M. Lockwood, B.J.I. Bromage, D.M. Willis and H. Lühr, The dependence of high-latitude dayside ionospheric flows on the north-south component of the IMF: a high time resolution correlation analysis using EISCAT "POLAR" and AMPTE UKS and IRM data, Planet. Space Sci., 36, 471 (1988)

14. A. Etemadi, S.W.H. Cowley and M. Lockwood, The effect of rapid changes in ionospheric flow on velocity vectors deduced from radar beam-swinging experiments, J. Atmos. Terr. Phys., submitted (1988)

15. H. Todd, S.W.H. Cowley, A. Etemadi, B.J.I. Bromage, M. Lockwood, D.M. Willis and H. Lühr, Flow in the high-latitude ionosphere: measurements at 15-second resolution made using the EISCAT "POLAR" experiment, J. Atmos. Terr. Phys., 50, 423 (1987)

16. J.R. Wygant, R.B. Torbert and F.S. Mozer, Comparison of S3-3 polar cap potential drops with the interplanetary magnetic field and models of magnetopause reconnection, J. Geophys. Res., 88, 5727 (1983)

17. T.E. Holzer, R.L. McPherron and D.A. Hardy, A quantitative emmpirical model of the magnetospheric flux transfer process, J. Geophys. Res., 91, 3287 (1986)

18. L.A. Frank, J.D. Craven, R.P. Lepping, C.T. Russell and E.J. Smith, Fluctuations of magnetotail energy in response to the solar wind, J. Geophys. Res., to be sumitted, (1988)

19. M. Lockwood and M.P. Freeman, Recent ionospheric observations relating to solar wind-magnetosphere coupling, Phil. Trans. Roy. Soc. (London), A, in press (1988)

20. G.L. Siscoe and T.S. Huang, Polar-cap inflation and deflation, J. Geophys. Res., 90, 543 (1985)

21. M. Lockwood, S.W.H. Cowley, M.P. Freeman, The excitation of ionospheric convection, J. Geophys. Res., to be submitted (1988)

22. D.J. Southwood, The ionospheric signature of flux transfer events, J. Geophys. Res., 92, 3207 (1987)

23. M. Lockwood, A.P. van Eyken, B.J.I. Bromage, J.H. Waite, Jr., T.E. Moore and J.R. Doupnik, Low-energy ion outflows from the ionosphere during a major cap expansion - evidence for equatorward motion of inverted-V structures, Adv. in Space Res., 6 (3), 93 (1986)

24. O. de la Beaujardiere, D.S. Evans, Y. Kamide, R.P. Lepping, Response of the auroral oval precipitation and magnetospheric convection to changes in the interplanetary magnetic field, Annales Geophys., 5A, 519 (1987)

25. C.R. Clauer, J.D. Kelly, M. Lockwood, R.M. Robinson, J.M. Ruohoniemi, O. de la Beaujardiere and L. Hakkinen, June 1987 GISMOS Experiment: preliminary report on high-time resolution, multi-radar measurements, Adv. in Space Res., in press (1988)

26. M. Lockwood, S.W.H. Cowley, H. Todd, D.M. Willis and C.R. Clauer, Ion flows and heating at a contracting polar-cap boundary, Planet. Space Sci., in press (1988)

27. I.G. Richardson, C.J. Owen, S.W.H. Cowley, A.B. Galvin, T.R. Sanderson, M. Scholer, J.A. Slavin and R.D. Zwickl, ISEE-3 observations during the CDAW-8 Intervals: Case studies if the distant geomagnetic tail covering a wide range of geomagnetic activity, J. Geophys. Res., submitted (1988)

28. W.J. Heikkila, Comment on Electric field evidence on the viscous interaction at the magnetopause, by F.S. Mozer, Geophys. Res. Lett., 13, 233 (1986)

29. W.J. Heikkila, Inductive electric field at magnetopause, Geophys. Res. Lett., 9, 877 (1982)

30. F.S. Mozer, Electric field evidence on the viscous interaction at the magnetopause, Geophys. Res. Lett., 11, 135 (1984)

31. F.S. Mozer, Reply, Geophys. Res. Lett., 13, 235 (1986)

32. W.R. Coley, R.A. Heelis, W.B. Hanson, P.H. Reiff, J.R. Sharber and J.D. Winningham, Ionospheric convection signatures and magnetic field topology, J. Geophys. Res., 92, 12352 (1987)

33. H. Todd, B.J.I. Bromage, S.W.H. Cowley, M. Lockwood, A.P. van Eyken and D.M. Willis, EISCAT observations of bursts of rapid flow in the high latitude dayside ionosphere, Geophys. Res. Lett., 13, 909 (1986)

34. M. Lockwood, M.F. Smith, C.J. Farrugia and G.L. Siscoe, Ionospheric ion upwelling in the wake of Flux Transfer Events at the dayside magnetopause, J. Geophys. Res., 93, 5641 (1988)

35. D.J. Southwood, C.J. Farrugia and M.A. Saunders, What are flux transfer events?, Planet. Space Sci., 36, 503 (1988)

36. P.E. Sandholt, IMF Control of the polar cusp aurora, Adv. in Space Res., this issue.

37. L.J. Lanzerotti, R.D. Hunsucker, D. Rice, L.C. Lee, A. Wolfe, C.G. Maclennan, and L.V. Medford, Ionosphere and ground-based response to field-aligned currents near magnetospheric cusp region, J. Geophys. Res., 92, 7739 (1987)

38. T. Oguti, T. Yamanoto, K. Hayashi, S. Kokubun, A. Egeland and J.A. Holtet, Dayside auroral activity and related magnetic impluses in the polar cap region, J. Geomag. Geoelect., 40, 387 (1988)

39. M.A. McHenry and C.R. Clauer, Modelled ground magnetic signatures of flux transfer events, J. Geophys. Res., 92, 11231 (1987)

40. K.-H. Glassmeier, M. Hoenisch and J. Untiedt, Ground-based and satellite observations of traveling magnetospheric covection twin-vortices J. Geophys. Res., in press, 1988.

41. E. Friis-Christensen, M.A. McHenry, C.R. Clauer and S. Vennerstrom, Ionospheric travelling convection vortices observed near the polar cleft: a triggered response to sudden changes in the solar wind, Geophys. Res. Lett., 15, 253 (1988)

42. M.A. McHenry, C.R. Clauer, E. Friis-Christensen, and J.D. Kelly, Observations of ionospheric convection vortices signatures of momentum transfer, Adv. in Space. Res., this issue.

43. T.A. Potemra, L.J. Zanetti, P.F. Bythrow, R.E. Earlandson, G.T. Markland, L.P. Block and H. Lühr, Multi-satellite and surface observations of geomagnetic field oscillations (co-incident AMPTE/CCE, VIKING, IMP-8 and EISCAT CROSS magnetic field observations), Adv. in space Res., this issue.

44. C.J. Farrugia, M.P. Freeman, S.W.H. Cowley, D.J. Southwood, M. Lockwood and A. Etemadi, Pressure-driven magnetopause motions and attendant response on the ground, Planet. Space Sci., submitted, 1988.

45. A. Nishida, Coherence of geomagnetic DP2 fluctuations with interplanetary magnetic variations, J. Geophys. Res., 73, 5549 (1968)

46. P.H. Reiff, R.W. Spiro, R.A. Wolfe, Y. Kamide, and J.H. King, Comparison of polar cap potential drops estimated from solar wind and ground magnetometer data: CDAW6, J. Geophys. Res., 90, 1318 (1985)

47. C.R. Clauer and E. Friis-Christensen, High-latitude dayside electric fields and currents during strong northward iterplanetary magnetic field : observations and model simulation, J. Geophys. Res., 93, 2749 (1988)

48. J.S. Murphree and R.D. Elphinstone, Correlative studies using the VIKING Imagery, Adv. in Space Res., this issue.

49. R.E. Holzer and J.A. Slavin, Magnetic flux transfer associated with expansions and contractions of the dayside magnetosphere, J. Geophys. Res., 83, 3831 (1978)

50. S. Kokubun, T. Yamamoto, K. Hayashi, T. Oguti and A. Egeland, Impulsive Pi bursts associated with poleward moving auroras near the polar cap, J. Geomag. Geoelectr., 40, 537 (1988)